The HKU Scholars Hub   The University of Hong Kong   香港大學學術庫

Title	Novel Hybrid Au/Fe3O4 Magnetic Octahedron-like Nanoparticles with Tunable Size
Author(s)	Li, L; Mak, KY; Leung, CW; Leung, CH; Ruotolo, A; Chan, GKY; Chan, WK; Pong, PWT
Citation	IEEE Transactions on Magnetics, 2014, v. 50 no. 1, article no. 2300405
Issued Date	2014
URL	http://hdl.handle.net/10722/185720
Rights	Creative Commons: Attribution 3.0 Hong Kong License

Novel Hybrid Au/Fe$_3$O$_4$ Magnetic Octahedron-like Nanoparticles with Tunable Size

L. Li[1], Y. M. Du[1] , K. Y. Mak[1] , C. W. Leung[2], and P. W. T. Pong[1]

[1]Department of Electrical and Electronic Engineering, The University of Hong Kong, Hong Kong
[2]Department of Applied Physics, Hong Kong Polytechnic University, Hong Kong

Octahedron-like Au/Fe$_3$O$_4$ magnetic nanoparticles are synthesized using decomposition of FeO(OH) and HAuCl$_4$ with the presence of oleic acid in 1-octadecene solvent. In the octahedron-like hybrid particles, Fe$_3$O$_4$ mainly displayed the octahedral morphology and spherical Au nanoparticles partially embedded into one side of Fe$_3$O$_4$ octahedron. The size of particle could be tuned from 25 to 240 nm for the whole particle (mainly for Fe$_3$O$_4$) and 10 to 40 nm for Au by changing the proportion of the starting materials. The hybrid particles showed the magnetic properties of Fe$_3$O$_4$ with dependence on the size of Fe$_3$O$_4$ octahedron composite and the proportion of Fe$_3$O$_4$ to Au. Coercivity is observed in the hybrid Au/Fe$_3$O$_4$ octahedron-like nanoparticles (55 Oe for 25 nm, 135 Oe for 100 nm, and 159 Oe for 240 nm) at room temperature. These size-controllable hybrid Au/Fe$_3$O$_4$ magnetic octahedron-like particles, inheriting the advantages of Au and Fe$_3$O$_4$ nanoparticles, may evolve as useful building blocks for nano- and micro-electronic applications.

Index Terms—Gold, hybrid nanoparticles, iron oxide, octahedron, tunable size.

I. INTRODUCTION

A RESEARCH topic of growing importance in nanomaterials synthesis is to design the systems possessing diverse physical and chemical properties through the assembling of different materials into hybrid nanostructures. The multicomponent nanostructures can inherit the chemical and physical properties of individual domains. In some cases, it can even provide entirely novel properties via the coupling between components, which will be essential for the future technological applications. For instance, the structural stability and fluorescence efficiency of semiconductor nanoparticle (CdSe) can be enhanced by the CdS or ZnS nanoshells [1], [2]. Besides the significant progress in the synthesis of hybrid semiconductor nanoparticles, a number of heterostructures that combine other materials has been successfully fabricated to date, including CoPt$_3$/Au dumbbells [3], Ru–Pt core–shell nanoparticles [4], Au/Pd nanooctahedron [5], Pd/Ag and Pt/Ag nanoboxes [6], Au/Fe$_3$O$_4$ dumbbells and "nanoflowers" [7], [8]. Among these binary hybrid nanomaterials, the combinations of gold and iron oxide have attracted increasing interests from material scientists because they are promising to inherit the advantageous properties from both individual gold and iron oxide nanoparticles.

The magnetic iron oxide-based materials often exhibit magnetic properties and can be used for selective capture of targeting molecules, recyclable nanocatalysis, magnetic bio-detection purposes, and magnetic resonance imaging (MRI) contrast enhancement [9]–[12]. The combination of gold and iron oxide can offer the promise of new application because of the complementary properties of gold to iron oxide. It has been found that the gold nanoshell can modulate the magnetic properties of iron oxide nanoparticles in iron oxide/gold core/shell structure [13]. The gold domains can facilitate chemical functionalization by using thiols or disulfides on gold/iron oxide hybrid dumbbell-like nanoparticles, and the bio-conjugated hybrid nanoparticles have great potential to serve as an effective antigen-targeted photothermal therapeutic agent for cancer treatment as well as a probe for magnetic resonance-based imaging [14]. For the preparation of binary gold/iron oxide hybrid nanoparticles, several methods have been reported, including thermal decomposition method, laser process method, and sonochemical methods [8], [15], [16]. Various morphologies of the hybrid nanoparticles have been realized, such as peanut-like, dumbbell-like, "nanoflower"-like, and sphere-like (core-shell or core-satellite structure) shapes [7], [8], [17]. Here, we report a straightforward and environmentally friendly approach to synthesizing binary Au/Fe$_3$O$_4$ magnetic nanoparticles with a novel octahedron-like morphology, consisting of spherical gold nanoparticles partially embedded into one side of the iron oxide octahedron. The synthetic procedure is inspired by the methods of Sun's group [8] and Colvin's group [18] and is based on the thermal decomposition of FeO(OH) and HAuCl$_4$ in the presence of oleic acid in high boiling-point solvent. The iron precursor (FeO(OH)) and gold precursor (HAuCl$_4$) are both environmentally friendly, nontoxic, and safe reagents. The sizes of the final Au/Fe$_3$O$_4$ hybrid products, especially the size of iron oxide octahedral component, can be adjusted by changing the proportion of starting materials. We characterize the synthesized particles using transmission electron microscopy (TEM), selected area electron diffraction pattern (SAEDP), scanning electron microscopy (SEM), energy-dispersive X-ray spectroscopy (EDS), and a vibrating sample magnetometer (VSM).

II. EXPERIMENT

A. Materials

Hydrated iron (III) oxide (FeO(OH)), Gold(III) chloride (HAuCl$_4$), oleic acid (OA), 1-octadecene, and dioctyl ether were purchased from Sigma-Aldrich (USA). All chemicals were used as received.

B. Synthesis of Au/Fe$_3$O$_4$ Hybrid Nanoparticles

All the nanoproducts were synthesized in a three-neck flask equipped with condenser, magnetic stirrer, thermocouple, and

heating mantle. Typically, a mixture of FeO(OH) fine powder, 2.26 g oleic acid, and 5 g 1-octadecene was stirred and heated to 120 °C under a gentle flow of nitrogen. During this period, the solution turned from turbid black to clear brown, and the iron oleate formed [18]. Then under a blanket of nitrogen, the gold precursor solution consisting of 0.068 g HAuCl$_4$ and 2 g dioctyl ether was injected into the solution. After maintaining 120 °C for 10 minutes, the mixture was heated to reflux ($\sim 310°C$) for 2 hours, cooled down to room temperature, and exposed to air for an extra 30 minutes to ensure the formation of Fe$_3$O$_4$. The final products were precipitated out of 1-octadecene by acetone, washed several times with 1:2 mixture of chloroform and acetone, extracted by magnetic attraction, and redispersed in chloroform. The amount of FeO(OH) was varied to prepare hybrid Au/Fe$_3$O$_4$ nanoparticles of different sizes. For comparison, the iron oxide nanoparticles (IONPs) were synthesized using the same synthetic process only without the presence of HAuCl$_4$.

C. Characterization

The size and morphology of the synthesized nanoparticles were examined under TEM (FEI Tecnai G2 20 S-TWIN) and SEM (Hitachi S-4800 FEG). The chemical components of the nanoparticles were analyzed through energy-dispersive X-ray spectroscopy (EDS) microanalysis. For TEM observation, samples were prepared by dispensing dilute drops of the nanoparticles chloroform suspension on carbon-coated copper grids and allowed to dry slowly. For SEM observation and EDS analysis, samples were prepared by dispensing one drop of the nanoparticles chloroform suspension on silicon wafer and allowed to dry slowly. The magnetic properties of nanoparticles were carried out using a VSM (Lakeshore, VSM 7400). The magnetization was measured over a range of applied field from -10 000 to 10 000 Oe.

III. RESULTS AND DISCUSSION

The as-synthesized gold/iron oxide hybrid nanoparticles (GIONPs) and its control IONPs displayed different morphologies and dimensions under TEM observation (Fig. 1). The initial molar ratio of FeO(OH)/HAuCl$_4$ in the experiment is denoted as R. Most GIONP products [Fig. 1(a)] synthesized when R = 10 mainly showed a quadrilateral morphology with mean size about 240 nm. As shown in the high-magnification view of one GIONP [inset in Fig. 1(a)], gold particle (~ 40 nm) appears black and iron oxide is light colored in the image because gold has a higher electron density and allows fewer electrons to transmit [8]. The corresponding IONP products [Fig. 1(b)] synthesized through the same synthetic route but without the presence of HAuCl$_4$ served as control. These IONPs have spherical morphology with uniform size of 13 nm. Fig. 1(c) is a typical high-resolution TEM (HRTEM) image of a single IONP. Fig. 1(a1), 1(b1), and 1(c1) shows the corresponding electron diffraction patterns of Fig. 1a, 1b, and 1c. The diffraction pattern in Fig. 1(a1) demonstrates that the iron oxide in GIONPs is magnetite (Fe$_3$O$_4$). The Au diffraction rings cannot be distinguished easily from the pattern because of the small volume fraction of Au in the GIONPs. Fig. 1(b1) shows a characteristic diffraction pattern of the Fe$_3$O$_4$ particles. Fig. 1(c1) confirms and reveals the single-crystal nature of IONP with the [1 1 1] zone axis. Two spacings of 0.29 nm are
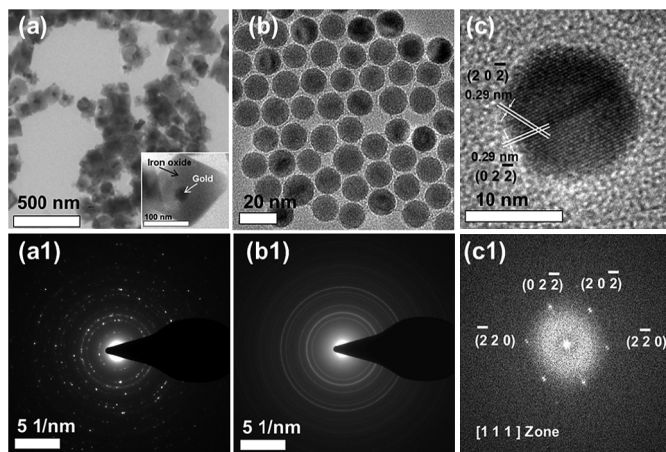

Fig. 1. TEM images of (a) hybrid Au/Fe$_3$O$_4$ nanoparticles (GIONPs, initial molar ratio R of FeO(OH)/HAuCl$_4$ = 10) and (b) iron oxide nanoparticles (IONPs, 13 nm). Inset in Fig. 1(a) is the high-magnification view of one GIONP. (c) HRTEM image of a single IONP. Electron diffraction pattern of (a1) GIONPs, (b1) IONPs, and (c1) single IONP.

consistent with the planes of $(2\,0\,\bar{2})$ and $(0\,2\,\bar{2})$ [19]. This result demonstrates that the introduction of gold precursor (HAuCl$_4$) into our reaction system induces dramatic changes on the size and morphology of final products. This should be attributed to the catalytic ability of gold nanoparticles on the decomposition of iron oleate. The catalytic ability of gold nanoparticles has been already used in the synthesis of hybrid gold/iron oxide nanoparticles with peanut-like, dumbbell-like, and core-shell structures [7], [8], [17]. In order to confirm the formation of gold nanoparticles in advance of the formation of iron oxide nanoparticles in our experiment, some reaction mixture was extracted when the reaction temperature reached 150 °C. Only gold nanoparticles were found in the mixture solution while no formation of iron oxide nanoparticles could be viewed under TEM observation. This confirmed that the gold nanoparticles were presynthesized before the decomposition of iron oleate into iron oxide nanoparticles.

To further study their morphology and their chemical components, the GIONP samples were analyzed by SEM and EDS (Fig. 2). We found that the increase of FeO(OH) precursor amount in the reaction system leads to the size increase of the final GIONP products. The mean sizes of GIONPs synthesized with varied amount of iron precursors are about 25 nm [GIONP-25, R = 2, Fig. 2(a)], 100 nm [GIONP-100, R = 5, Fig. 2(b)], and 240 nm [GIONP-240, R = 10, Fig. 2(c)], respectively. Different from the peanut-like, dumbbell-like, "nanoflower"-like, and nanoporous core/shell spherical shapes of the gold/iron oxide hybrid nanoparticles which have already been fabricated by other research groups [7], [8], [17], the GIONP products obtained in our experiments displayed a new octahedron-like shape [as illustrated by the red octahedron schematic plots in Fig. 2(a), Fig. 2(b), and Fig. 2(c)]. Fig. 2(d) is a representative EDS result of GIONP-240. The elements of Fe and Au are confirmed in all the GIONP products.

As shown in the TEM images (Fig. 3), GIONP-25 [R = 2, Fig. 3(a)], GIONP-100 [R = 5, Fig. 3(b)] and GIONP-240 [R = 10, Fig. 3(c)] displayed increased size as the iron precursor increased. This is consistent with the observation in the SEM images (Fig. 2). The quadrilateral and hexagonal images
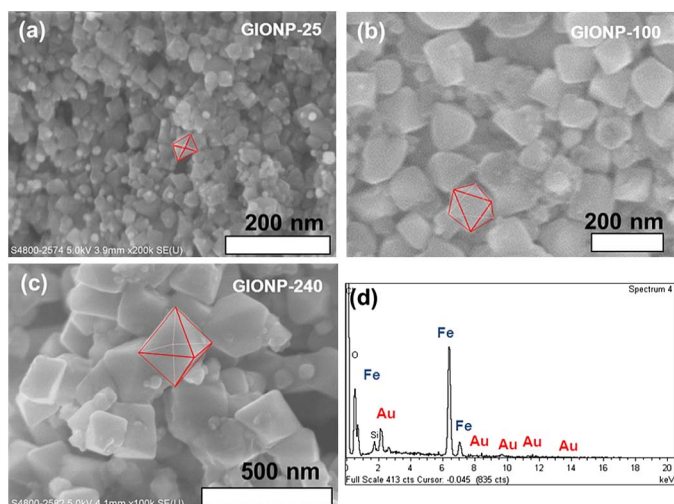
Fig. 2 (Color online) SEM images of (a) GIONP-25, hybrid Au/Fe$_3$O$_4$ nanoparticles with initial molar ratio R of FeO(OH)/HAuCl$_4$ = 2, (b) GIONP-100, hybrid Au/Fe$_3$O$_4$ nanoparticles with initial molar ratio R of FeO(OH)/HAuCl$_4$ = 5, and (c) GIONP-240, hybrid Au/Fe$_3$O$_4$ nanoparticles with initial molar ratio R of FeO(OH)/HAuCl$_4$ = 10. Red octahedral schematic plots are provided as visual guides. (d) EDS result of GIONP-240. Elements of Fe and Au are labeled.

Fig. 3 (Color online) TEM images of (a) GIONP-25, hybrid Au/Fe$_3$O$_4$ nanoparticles with initial molar ratio R of FeO(OH)/HAuCl$_4$ = 2, (b) GIONP-100, hybrid Au/Fe$_3$O$_4$ nanoparticles with initial molar ratio R of FeO(OH)/HAuCl$_4$ = 5, and (c) GIONP-240, hybrid Au/Fe$_3$O$_4$ nanoparticles with initial molar ratio R of FeO(OH)/HAuCl$_4$ = 10. Red octahedron in Fig. 3(a) represents the corresponding 3-D schematic models of the hexagonal 2-D projection of GIONPs. (d) 3-D schematic models for the GIONP-25. In this octahedron-like particle, one spherical Au nanoparticle partially embedded into one face of the Fe$_3$O$_4$ octahedron.

of the GIONPs under TEM observation are the 2-D projection of the octahedron through different projection directions. The red octahedron in Fig. 3(a) represents the corresponding 3-D schematic models of the hexagonal 2-D projection of GIONPs. In addition, it can be observed that the gold nanoparticles are not located at the center of the iron oxide nanoparticles, and part of the gold nanoparticles extrude beyond the iron oxide nanoparticles area. This indicates that our GIONP-25 products do not have a core-sell structure but have a structure like the 3-D schematic model as shown in Fig. 3(d). In this structure, iron oxide nanoparticles maintain octahedral shape and part of the gold nanoparticles embedded on one face of the iron oxide octahedral nanoparticles. The sizes of gold nanoparticles in GIONP-100 (Au: 22 nm) and in GIONP-240 (Au: 40 nm) are much smaller than the respective iron oxide composites. Thus it is difficult to know if the gold nanoparticle is the wholly embedded or partly embedded inside the iron oxide octahedron from the electron microscopy images. Since this kind of composite structure is relatively novel, there is no well-established mechanism explaining their formation. Nevertheless, the final structure of hybrid particles seems to depend on whether the gold surface allows only a single nucleation site or multiple ones for iron oxide, which is related to the polarity of solvent used in the experiment [8]. For example, hybrid gold/iron oxide products can form core-shell structures in benzyl ether and phenyl ether. In contrast, iron oxide may only grow from a single site on gold surface in dioctyl ether and 1-octadecene. Since the solvent used in our experiment is dioctyl ether and 1-octadecene, we presume that the iron oxide cannot grow around the gold nanoparticles. Thus, the morphologies of GIONP-100 and GIONP-240 are likely to develop the same structure [Fig. 3(d)] as GIONP-25, which needs to be further confirmed. In addition, the gold/magnetite interface in GIONPs is likely due to the phenomenon that the iron oxide starts to nucleate on a gold nanoparticle, and the shape of iron oxide crystals is mostly determined by the relative growth rates along
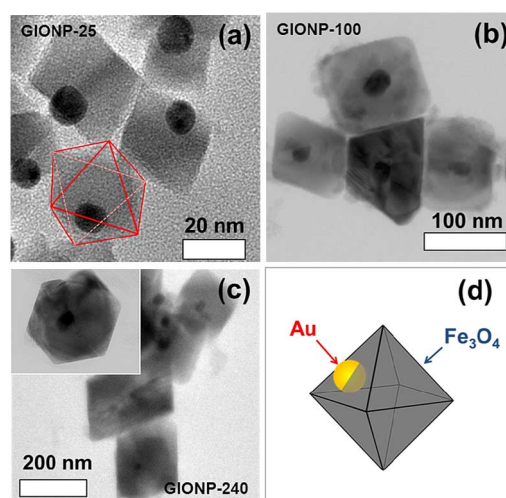
different directions [8], [20]. It is suggested that the shape of an fcc crystal, like magnetite, is mainly determined by the ratio of the growth rate in the ⟨100⟩ direction to that in the ⟨111⟩ direction [21]. Since the catalysis ability of gold nanoparticles played an important role in the formation of magnetite octahedral, we conjecture that the influence of gold nanoparticles may cause the growth rate of ⟨100⟩ planes to be higher than that of ⟨111⟩ planes, thus the shape of octahedron forms naturally [20].

The magnetic properties of the IONPs and GIONPs were characterized using VSM at room temperature (Fig. 4). The saturation magnetization (M$_S$) for IONPs, GIONP-25, GIONP-100, and GIONP-240 are 60, 30, 42, and 55 emu/g, respectively. The M$_S$ values of three GIONPs samples are all less than the M$_S$ of IONPs due to the presence of the nonmagnetic gold in the samples, but are much larger than the M$_S$ value ($\sim$ 5 emu/g) of the gold/magnetite nanocomposites formed via sonochemical methods [22]. Meanwhile, the M$_S$ values of the GIONP-25, GIONP-100, and GIONP-240 are 30, 42, and 55 emu/g, respectively, indicating the M$_S$ of the samples increases with the sample size. This phenomenon can be explained by two reasons. First, the increase of FeO(OH) precursor amount in reaction system leads to the size increase of GIONPs, along with the size increase of their iron oxide composites, as shown in TEM image (Fig. 3). Since the M$_S$ value of IONPs increases in proportion to the particle size in the nanometer regime [23] higher M$_S$ value exists in the iron oxide composite with larger size. Thus, the size-dependent M$_S$ value of the GIONPs can be partly attributed to the increasing M$_S$ value with the increasing size of its iron oxide composite. Second, the initial molar ratio of iron-precursor/gold-precursor (FeO(OH)/HAuCl$_4$) is R = 2, R = 5, and R = 10 for the GIONP-25, GIONP-100, and GIONP-240, respectively. With higher R value used, the size of GIONPs increases, along with the higher the proportion of magnetic iron oxide obtained in the corresponding GIONPs, and larger M$_S$ value can be expected.
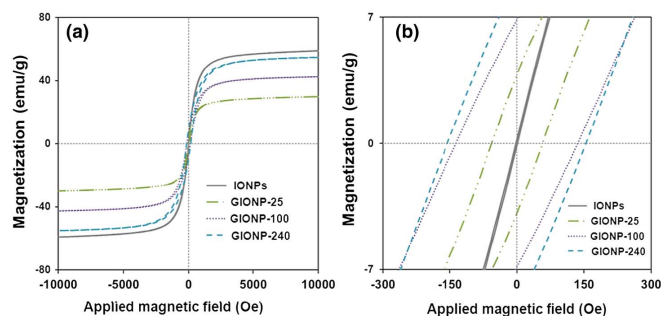
Fig. 4 (Color online) (a) Full view of magnetization curve and (b) magnified views of the M-H loops in the low magnetic field of iron oxide nanoparticles (IONPs, 13 nm), hybrid Au/Fe_3O_4 nanoparticles with initial molar ratio R of $FeO(OH)/HAuCl_4 = 2$ (GIONP-25), hybrid Au/Fe_3O_4 nanoparticles with initial molar ratio R of $FeO(OH)/HAuCl_4 = 5$ (GIONP-100), and hybrid Au/Fe_3O_4 nanoparticles with initial molar ratio R of $FeO(OH)/HAuCl_4 = 10$ (GIONP-240).

As such, the increasing trend of M_S value in GIONP-25, GIONP-100, and GIONP-240 can be attributed to the increased ratio of magnetic iron oxide to nonmagnetic gold in the final products. The magnified views of the M-H loops in the low magnetic field are shown in Fig. 4b. The IONPs show super-paramagnetic behavior with no coercivity. The coercivity of GIONP-25 is 55 Oe, comparable with the coercivity of 25 nm iron oxide nanoparticles (45 Oe) [24]. This is mainly because the iron oxide octahedron composites in GIONPs have a size of around 25 nm. As the size of hybrid Au/Fe_3O_4 octahedron-like particles increases to 100 nm and 240 nm, the coercivities of particles increase to 135 Oe (GIONP-100) and 159 Oe (GIONP-240). Thus, the GIONP samples showed size-dependent coercivity, which can be explained by the random anisotropy model [25]. The degree of magnetic anisotropy increases with the size of iron oxide particle, which leads to higher coercivity [26]. Therefore, the larger the size of the GIONP samples, the larger the size of the iron oxide composite, which is responsible for the higher coercivity value. The increasing coercivity with particle size is consistent with the phenomena reported in magnetite nanoparticles [27]. In addition, the GIONP-100 and GIONP-240 showed coercivities of 135 Oe and 159 Oe, larger than the coercivities of spherical iron oxide nanoparticles with similar sizes of 81 nm (89 Oe) and 282 nm (62 Oe) [27]. This is because the coercivity of magnetite is governed by the particle shape and it is larger in the octahedral particles than in the spherical ones [28].

IV. CONCLUSION

Here, we have reported a simple and environmentally friendly approach to synthesize binary Au/Fe_3O_4 magnetic nanoparticles with a novel octahedron-like morphology, consisting of gold nanoparticles partially embedded into one side of iron oxide octahedron. The sizes of the binary products, especially the iron oxide octahedral component, can be adjusted by changing the proportion of starting materials. Magnetic measurements indicate the hybrid Au/Fe_3O_4 magnetic octahedron-like particles showed the magnetic behavior like their Fe_3O_4 components. The exposed part of the gold surface can be used for attachment of thiol-terminated molecules, especially biomolecules. The magnetic behavior of Fe_3O_4 provides the hybrid products with the potential to be used as magnetic labels

which can be detected by magnetic sensors or captured by magnetic field. With the novel morphology and tunable sizes from 25 to larger than 200 nm, hybrid Au/Fe_3O_4 magnetic octahedron-like particles may evolve as useful building blocks for nano-/micro-electronic application.

REFERENCES

[1] M. A. Hines and P. Guyot-Sionnest, "Synthesis and characterization of strongly luminescing ZnS-capped CdSe nanocrystals," *J. Phys. Chem.*, vol. 100, pp. 468–471, 1996.

[2] X. Peng, M. C. Schlamp, A. V. Kadavanich, and A. Alivisatos, "Epitaxial growth of highly luminescent CdSe/CdS core/shell nanocrystals with photostability and electronic accessibility," *J. Amer. Chem. Soc.*, vol. 119, pp. 7019–7029, 1997.

[3] T. Pellegrino, A. Fiore, E. Carlino, C. Giannini, P. D. Cozzoli, G. Ciccarella, M. Respaud, L. Palmirotta, R. Cingolani, and L. Manna, "Heterodimers based on $CoPt_3$-Au nanocrystals with tunable domain size," *J. Amer. Chem. Soc.*, vol. 128, pp. 6690–6698, 2006.

[4] S. Alayoglu, A. U. Nilekar, M. Mavrikakis, and B. Eichhorn, "Ru–Pt core–shell nanoparticles for preferential oxidation of carbon monoxide in hydrogen," *Nature Mat.*, vol. 7, pp. 333–338, 2008.

[5] Y. W. Lee, M. Kim, Z. H. Kim, and S. W. Han, "One-step synthesis of Au@Pd core–shell nanooctahedron," *J. Amer. Chem. Soc.*, vol. 131, pp. 17036–17037, 2009.

[6] J. Chen, B. Wiley, J. McLellan, Y. Xiong, Z.-Y. Li, and Y. Xia, "Optical properties of Pd-Ag and Pt-Ag nanoboxes synthesized via galvanic replacement reactions," *Nano Lett.*, vol. 5, pp. 2058–2062, 2005.

[7] Y. Wei, R. Klajn, A. O. Pinchuk, and B. A. Grzybowski, "Synthesis, shape control, and optical properties of hybrid Au/Fe_3O_4 "nanoflowers"," *Small*, vol. 4, pp. 1635–1639, 2008.

[8] H. Yu, M. Chen, P. M. Rice, S. X. Wang, R. L. White, and S. Sun, "Dumbbell-like bifunctional $Au − Fe_3O_4$ nanoparticles," *Nano Lett.*, vol. 5, pp. 379–382, 2005.

[9] J.-H. Lee, Y.-M. Huh, Y.-w. Jun, J.-w. Seo, J.-t. Jang, H.-T. Song, S. Kim, E.-J. Cho, H.-G. Yoon, and J.-S. Suh, "Artificially engineered magnetic nanoparticles for ultra-sensitive molecular imaging," *Nature Med.*, vol. 13, pp. 95–99, 2006.

[10] A. K. Gupta and M. Gupta, "Synthesis and surface engineering of iron oxide nanoparticles for biomedical applications," *Biomaterials*, vol. 26, pp. 3995–4021, 2005.

[11] G. Lee, J. Kim, and J.-h. Lee, "Development of magnetically separable polyaniline nanofibers for enzyme immobilization and recovery," *Enzyme Microbial Technol.*, vol. 42, pp. 466–472, 2008.

[12] R. S. Gaster, L. Xu, S.-J. Han, R. J. Wilson, D. A. Hall, S. J. Osterfeld, H. Yu, and S. X. Wang, "Quantification of protein interactions and solution transport using high-density GMR sensor arrays," *Nature Nanotechnol.*, vol. 6, pp. 314–320, 2011.

[13] S. Banerjee, S. Raja, M. Sardar, N. Gayathri, B. Ghosh, and A. Dasgupta, "Enhanced magnetism, memory and aging in Gold-Iron oxide nanoparticle composites," arXiv preprint arXiv:0906.1497 2009.

[14] D. K. Kirui, D. A. Rey, and C. A. Batt, "Gold hybrid nanoparticles for targeted phototherapy and cancer imaging," *Nanotechnol.*, vol. 21, p. 105105, 2010.

[15] K. Kawaguchi, J. Jaworski, Y. Ishikawa, T. Sasaki, and N. Koshizaki, "Preparation of gold/iron-oxide composite nanoparticles by a unique laser process in water," *J. Magnetism Magn. Mat.*, vol. 310, pp. 2369–2371, 2007.

[16] W. Wu, Q. He, H. Chen, J. Tang, and L. Nie, "Sonochemical synthesis, structure and magnetic properties of air-stable Fe_3O_4/Au nanoparticles," *Nanotechnol.*, vol. 18, p. 145609, 2007.

[17] E. V. Shevchenko, M. I. Bodnarchuk, M. V. Kovalenko, D. V. Talapin, R. K. Smith, S. Aloni, W. Heiss, and A. P. Alivisatos, "Gold/Iron oxide core/hollow-shell nanoparticles," *Adv. Mat.*, vol. 20, pp. 4323–4329, 2008.

[18] W. Y. William, J. C. Falkner, C. T. Yavuz, and V. L. Colvin, "Synthesis of monodisperse iron oxide nanocrystals by thermal decomposition of iron carboxylate salts," *Chem. Commun.*, pp. 2306–2307, 2004.

[19] Y. L. Chueh, M. W. Lai, J. Q. Liang, L. J. Chou, and Z. L. Wang, "Systematic study of the growth of aligned arrays of α-Fe$_2$O$_3$ and Fe$_3$O$_4$ nanowires by a vapor–solid process," *Adv. Functional Mat.*, vol. 16, pp. 2243–2251, 2006.

[20] E. C. Stoner and E. Wohlfarth, "A mechanism of magnetic hysteresis in heterogeneous alloys," *Philosophical Transactions of the Royal Soc. of London. Series A. Mathematical and Phys. Sci.*, pp. 599–642, 1948.

[21] Z. Wang, "Transmission electron microscopy of shape-controlled nanocrystals and their assemblies," *J. Phys. Chem. B*, vol. 104, pp. 1153–1175, 2000.

[22] A. Pradhan, R. C. Jones, D. Caruntu, C. J. O'Connor, and M. A. Tarr, "Gold–Magnetite nanocomposite materials formed via sonochemical methods," *Ultrason. Sonochemistry*, vol. 15, pp. 891–897, 2008.

[23] K. Nogi, M. Hosokawa, M. Naito, and T. Yokoyama, *Nanoparticle Technol. Handbook*. New York, NY, USA: Elsevier Science, 2012.

[24] L. Li, K. Mak, J. Shi, H. Koon, C. Leung, C. Wong, C. Leung, C. Mak, N. Chan, and W. Zhong, "Comparative in vitro cytotoxicity study on uncoated magnetic nanoparticles: Effects on cell viability, cell morphology, and cellular uptake," *J. Nanosci. and Nanotechnol.*, vol. 12, pp. 9010–9017, 2012.

[25] G. Herzer, "Grain size dependence of coercivity and permeability in nanocrystalline ferromagnets," *IEEE Trans. Magn.*, vol. 26, no. 4, pp. 1397–1402, Jul. 1990.

[26] C. C. Ferraioli and V. U. Chemistry, *Nanocrystals, Core-Shells, and Nanocapsules of Iron Oxide*. Philadelphia, PA, USA: Villanova Univ., 2008.

[27] M. Ma, Y. Wu, J. Zhou, Y. Sun, Y. Zhang, and N. Gu, "Size dependence of specific power absorption of Fe$_3$O$_4$ particles in AC magnetic field," *J. Magnetism Magn. Mat.*, vol. 268, pp. 33–39, 2004.

[28] A. S. Teja and P.-Y. Koh, "Synthesis, properties, and applications of magnetic iron oxide nanoparticles," *Progress in Crystal Growth Characterization Mat.*, vol. 55, pp. 22–45, 2009.